ChemComm

COMMUNICATION

View Article Online
View Journal | View Issue

A new metal–organic framework with ultra-high surface area†

Cite this: *Chem. Commun.*, 2014, **50**, 3450

Received 6th January 2014,
Accepted 4th February 2014

DOI: 10.1039/c4cc00113c

www.rsc.org/chemcomm

Ronny Grünker,[a] Volodymyr Bon,[a] Philipp Müller,[a] Ulrich Stoeck,[a] Simon Krause,[a] Uwe Mueller,[b] Irena Senkovska[a] and Stefan Kaskel*[a]

A new mesoporous MOF, $Zn_4O(bpdc)(btctb)_{4/3}$ (DUT-32), containing linear ditopic ($bpdc^{2-}$; 4,4′-biphenylenedicarboxylic acid) and tritopic ($btctb^{3-}$; 4,4′,4″-[benzene-1,3,5-triyltris(carbonylimino)]tris-benzoate) linkers, was synthesised. The highly porous solid has a total pore volume of 3.16 $cm^3\ g^{-1}$ and a specific BET surface area of 6411 $m^2\ g^{-1}$, adding this compound to the top ten porous materials with the highest BET surface area.

During the last two decades metal–organic frameworks (MOFs) have continuously set new records in terms of specific surface area and pore volume, pushing the high pressure storage capacity for energetic molecules such as hydrogen and methane further and further.[1]

In order to avoid the disadvantageous formation of interpenetrated structures we propose the use of two different types of elongated linkers, one with a polar functionality, and another with a purely aromatic core structure. In the following we will show that this concept leads to a highly porous non-interpenetrated MOF structure but requires a distinct activation procedure due to the stronger interaction forces between solvating molecules and the polar functional groups of one linker.

As the polar tritopic linker 4,4′,4″-[benzene-1,3,5-triyltris-(carbonylimino)]trisbenzoic acid (H_3btctb), which has been very successfully applied in the synthesis of porous MOFs,[2] was used. 4,4′-Biphenylenedicarboxylic acid (H_2bpdc) was chosen as the more hydrophobic linker because of the ideal di- and tritopic linker length ratio (L_D/L_T) of 0.63. According to Matzger *et al.*, for the formation of copolymerization MOFs, the geometric factor describing the length ratio of the linkers as well as the connectivity to the cluster plays a key role in the formation of the given structure.[3] For known MOFs the L_D/L_T ratios lie within a region from 0.44 to 0.66 (Table S1, ESI†).

The solvothermal reaction of H_3btctb and H_2bpdc with zinc nitrate yields coffin-shaped transparent crystals of $Zn_4O(bpdc)(btctb)_{4/3}$ (DUT-32, DUT – Dresden University of Technology), while an excess of H_3btctb or H_2bpdc in the reaction mixture leads to the formation of byproducts: $Zn_4O(btctb)_2$ (DUT-59), $Zn_4O(btctb)_2(DMF)(H_2O)_{1.5}$ (ref. 2a) or $Zn_4O(bpdc)_3$ (IRMOF-10).[4] DUT-59 is isoreticular to MOF-177[5] (for more details see ESI†).

Interestingly, DUT-32 has a framework isorecticular to UMCM-2[6] with a rare **umt** topology crystallizing in the $P6_3/m$ space group.‡ The phase purity of bulk samples of DUT-32 was confirmed by powder X-ray diffraction measurements (see ESI†). The overall composition of the solvated material was determined by thermal (Fig. S7, ESI†) and elemental analysis, as well as ^{1}H-NMR (Fig. S8, ESI†), and can be described as $Zn_4O(bpdc)(btctb)_{4/3}(DEF)_{39.7}(H_2O)_{11.3}$.

The structure of DUT-32 consists of two symmetry-independent Zn_4O^{6+} octahedral secondary building units. Both of them are surrounded by four $btctb^{3-}$ and two $bpdc^{2-}$ linkers. The ditopic $bpdc^{2-}$ ligands at the first Zn_4O^{6+} cluster are arranged in a *trans* orientation, while the *cis* orientation of linkers relative to each other is found at the second cluster (Fig. 1 and Fig. S5, ESI†). With these types of connectivity, a 3D framework is constructed with

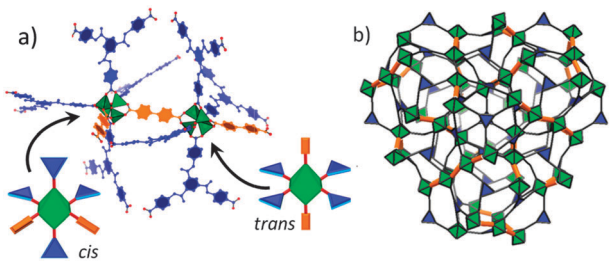

Fig. 1 (a) Two crystallographically independent diastereomeric SBUs in DUT-32; (b) simplified representation of DUT-32. Cluster – green, tritopic linker – blue, ditopic linker – orange.

[a] *Department of Inorganic Chemistry, Technische Universität Dresden, Bergstrasse 66, D-01069 Dresden, Germany. E-mail: stefan.kaskel@chemie.tu-dresden.de*
[b] *Helmholtz-Zentrum Berlin für Materialien und Energie, BESSY-MX Group, Albert-Einstein-Strasse 15, D-12489 Berlin, Germany*

† Electronic supplementary information (ESI) available: Synthetic details, single crystal X-ray structure analysis details, PXRD patterns, thermogravimetric analysis and NMR data. CCDC 968887 and 968888. For ESI and crystallographic data in CIF or other electronic format see DOI: 10.1039/c4cc00113c

three different but huge mesopores (30 × 40 Å, 28 × 32 Å and 20 × 26 Å, considering van der Waals radii of the atoms), and one smaller micropore (14 × 18 Å) (Fig. S1 and S2, ESI†). The crystallographic density of the desolvated DUT-32 is extremely low, only 0.27 g cm^{-3}, and is close to the density of MOF-210 (0.25 g cm^{-3}).[7]

However, not only the crystallographic porosity, but also real gas accessible volume of the compound generated after removal of solvent molecules are crucial for the manufacture of porous materials for numerous areas of application. Activation of DEF-containing DUT-32 samples by conventional heating under vacuum results in a non-porous materials. Similar results were observed for the solvent-exchange activation method using dichloromethane, chloroform or alcohols like methanol or ethanol.

For supercritical drying, the amide solvent incorporated into the pores was exchanged first with absolute ethanol, which shows high miscibility with liquid CO_2 and is commonly used for MOF activation. The resulting material exhibits an unexpected type IV nitrogen physisorption isotherm and relatively low BET surface area (838 m^2 g^{-1}) and micropore volume (0.36 cm^3 g^{-1}) (Fig. S9, ESI†) indicating a network distortion. However, a very high total pore volume of 2.91 cm^3 g^{-1} was calculated. PXRD measurements performed for the sample after drying indicate a complete loss of crystallinity.

Interestingly, a resolvation of this amorphous material with DEF and heating at 373 K for one day restores the crystallinity partly (Fig. S6a, ESI†). We suggest that due to its ability to form hydrogen bonds, ethanol binds quite strongly to the amide moieties of the network. Therefore, a complete exchange of the ethanol by CO_2 within the pores does not occur, leading to a structural rearrangement with a loss of crystallographically defined porosity during removal of residual ethanol. A complete structural collapse of the network probably does not occur because of the extremely high total pore volume which is close to the theoretical value of 3.21 cm^3 g^{-1}, the completely intact morphology of the dried crystals and the recovery of the network by resolvation.

For the supercritical drying process the choice of the solvent is mainly based on its miscibility with liquid CO_2.[8,9] Therefore, the influence of solvents with minor polarity on the porosity was investigated. Applying the same drying protocol but using anhydrous acetone instead of ethanol on the same material (sample mass 100 mg) with a resting time in CO_2 of one day (replacing the liquid CO_2 3 times a day) resulted in a material with completely different textural properties. PXRD measurements show that the crystallinity of the sample remains intact (Fig. S6, ESI†). This is also reflected in the N_2 physisorption isotherm which shows a typical shape for a MOF material with small mesopores and reaches saturation at 935 cm^3 g^{-1}, indicating a total pore volume of 1.44 cm^3 g^{-1} (Fig. S9b, ESI†).

However, this value remains too low in comparison to the geometrically calculated pore volume of 3.21 cm^3 g^{-1}, indicating insufficient activation. Interestingly, upon decreasing the amount of the sample for SCD drying from 100 mg to 30 mg and keeping the resting time in liquid CO_2 and replacement cycles the same (one day, three times a day, respectively), a sample with a significantly enhanced porosity was obtained. The adsorbed N_2 volume reaches a value of 1470 cm^3 g^{-1} representing a total pore volume of 2.27 cm^3 g^{-1} (Fig. S9b, ESI,† circles). Similar results can be observed by using amyl acetate instead of acetone indicating that for larger amounts of the sample the solvent exchange process with liquid CO_2 takes more time. These results show that the MOF/liquid_CO_2 ratio as well as resting time in liquid CO_2 (or corresponding CO_2 exchange frequency) have a crucial impact on the textural properties of DUT-32.

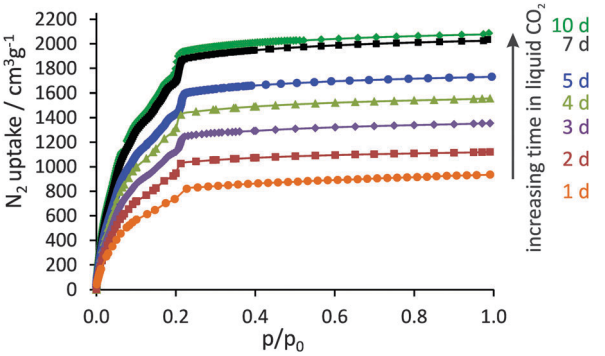

Fig. 2 N_2 physisorption isotherms at 77 K of DUT-32 after supercritical drying from amyl acetate as solvent with different resting times in liquid CO_2 during the drying process.

It could be shown that by systematically extending the resting time in liquid CO_2 (and exchange frequency), the porosity of DUT-32 can be significantly improved, finally reaching the theoretical limit (Fig. 2). The nitrogen uptake at 77 K increases steadily from 935 cm^3 g^{-1} (one day in liquid CO_2) up to a maximum of 2040 cm^3 g^{-1} (seven days in liquid CO_2). The maximum value corresponds to a specific pore volume of 3.16 cm^3 g^{-1}, which is remarkable. A further increase of exchange time to ten days showed only a slight porosity improvement with an adsorbed volume of nitrogen of 2080 cm^3 g^{-1}.

Applying consistency criteria suggested by Rouquerol and Llewellyn[10] to the N_2 physisorption isotherm for a sample with a resting time of seven days in liquid CO_2 (further denoted as DUT-32_7d) results in an apparent BET surface area as high as 6411 m^2 g^{-1} (see ESI†). This value is close to the geometrical surface area of DUT-32 calculated using the Poreblazer V1.2 program[11] (5981 m^2 g^{-1}). Additionally, the nitrogen adsorption isotherm was simulated using multipurpose simulation code MUSIC.[12] The simulated isotherm fits well with the experimental one (Fig. S13, ESI†). By applying the BET theory to the simulated isotherm in the same relative pressure region as for the experimental one (p/p_0 0.09–0.13), the surface area of 6255 m^2 g^{-1} was calculated.

DUT-32 also has excellent gas storage properties. For H_2 the excess maximum capacity is achieved at 53 bar and reaches 85 mg g^{-1} (7.8 wt%; 22.9 mg cm^{-3}) (Fig. 3) which is only surpassed by MOF-210 (86 mg g^{-1})[7] and NU-100 (99.5 mg g^{-1}).[13] Considering the enormous pore volume, the total capacity at 80 bar corresponds to 166 mg g^{-1} (14.21 wt%; 44.9 mg cm^{-3}) which is among the highest gravimetric values reported for porous materials.

Recently Yildirim *et al.*[1c] claimed that a hypothetical MOF with optimal methane storage properties should have a pore

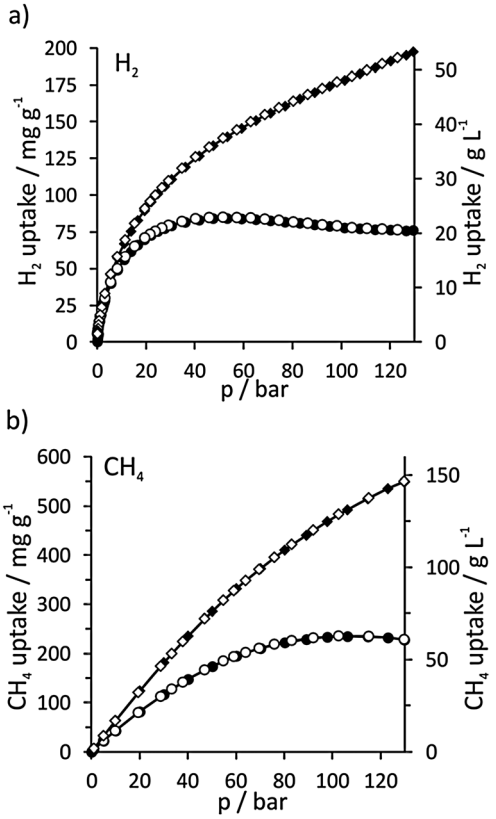

Fig. 3 H_2 (a, 77 K) and CH_4 (b, 298 K) physisorption isotherms of DUT-32_7d; excess (●), total (◆); filled and empty symbols correspond to the adsorption and desorption, respectively.

volume of 3.2 $cm^3\ g^{-1}$, a density of 0.27 g cm^{-3} and a surface area of 7500 $m^2\ g^{-1}$ to be able to adsorb 0.5 g methane per gram of MOF (195 cc (STP) cc^{-1}) at 65 bar. Interestingly, DUT-32 has the porosity characteristics which are very close to those of the desired hypothetical MOF: pore volume of 3.16 $cm^3\ g^{-1}$ and density of 0.27 g cm^{-3}. DUT-32's maximum excess methane capacity at 298 K is reached with 0.24 g g^{-1} at 105 bar (corresponding to 65 mg ml^{-1}). Due to the large pore volume, DUT-32 achieves a total desired CH_4 storage capacity of 0.55 g g^{-1} (149 g L^{-1}, 210 cm^3 (STP) cm^{-3}) at 130 bar.

Summarizing, we have presented a new metal–organic framework (DUT-32) with a rare **umt** topology that can be easily scaled up due to the simple linker synthesis using cheap starting materials. Careful adjustment of the activation conditions revealed an ultrahigh porosity with a nitrogen uptake of 2080 $cm^3\ g^{-1}$ (STP) corresponding to a total pore volume of 3.16 $cm^3\ g^{-1}$ and an apparent BET area of 6411 $m^2\ g^{-1}$, adding this compound to the top ten materials with the highest BET surface area.

The authors are grateful for the financial support from the DFG (SPP 1362), and the HZB. Special thanks goes to Dr G. Auffermann for carrying out the elemental analyses, and Dr I. Baburin for simulations.

Notes and references

‡ Crystallographic data: $C_{252.5}H_{491.3}N_{68}O_{43.7}Zn_4$, M = 5441.09 g mol^{-1}, hexagonal, $P6_3/m$ (Nr. 176), a = 50.710(7) Å, c = 62.920(13) Å, V = 140 122(40) $Å^3$, Z = 18, $\rho_{calc.}$ = 1.161 g cm^{-3}, λ = 0.88561 Å, T = 293 K, $2\theta_{max}$ = 28.2°, reflections collected/unique 118 656/60 048, R_{int} = 0.0497, R_1 = 0.0688, wR_2 = 0.1815, S = 1.010, largest diff. peak 0.229 e $Å^{-3}$ and hole −0.196 e $Å^{-3}$. CCDC 968887.

1 (*a*) H. Frost, T. Düren and R. Q. Snurr, *J. Phys. Chem. B*, 2006, **110**, 9565; (*b*) H. Frost and R. Q. Snurr, *J. Phys. Chem. C*, 2007, **111**, 18794; (*c*) Y. Peng, V. Krungleviciute, I. Eryazici, J. T. Hupp, O. K. Farha and T. Yildirim, *J. Am. Chem. Soc.*, 2013, **135**, 11887; (*d*) J. A. Mason, M. Veenstra and J. R. Long, *Chem. Sci.*, 2014, **5**, 32.
2 (*a*) X. Song, Y. Zou, X. Liu, M. Oh and M. S. Lah, *New J. Chem.*, 2010, **34**, 2396; (*b*) R. Ma, C. Chen, B. Sun, X. Zhao and N. Zhang, *Inorg. Chem. Commun.*, 2011, **14**, 1532; (*c*) S. Banerjee, N. N. Adarsh and P. Dastidar, *Soft Matter*, 2012, **8**, 7623; (*d*) Y. Zhang, Q. Wang, Y.-J. Xiao, J. Han and X.-L. Zhao, *Polyhedron*, 2012, **33**, 127; (*e*) L. Rajput, D. Kim and M. S. Lah, *CrystEngComm*, 2013, **15**, 259; (*f*) Y.-Q. Chen, S.-J. Liu, Y.-W. Li, G.-R. Li, K.-H. He, Z. Chang and X.-H. Bu, *CrystEngComm*, 2013, **15**, 1613.
3 K. Koh, A. G. Wong-Foy and A. J. Matzger, *J. Am. Chem. Soc.*, 2010, **132**, 15005.
4 M. Eddaoudi, J. Kim, N. Rosi, D. Vodak, J. Wachter, M. O'Keeffe and O. M. Yaghi, *Science*, 2002, **295**, 469.
5 H. K. Chae, D. Y. Siberio-Perez, J. Kim, Y. Go, M. Eddaoudi, A. J. Matzger, M. O'Keeffe and O. M. Yaghi, *Nature*, 2004, **427**, 523–527.
6 K. Koh, A. G. Wong-Foy and A. J. Matzger, *J. Am. Chem. Soc.*, 2009, **131**, 4184.
7 H. Furukawa, N. Ko, Y. B. Go, N. Aratani, S. B. Choi, E. Choi, A. O. Yazaydin, R. Q. Snurr, M. O'Keeffe, J. Kim and O. M. Yaghi, *Science*, 2010, **329**, 424.
8 J. E. Mondloch, O. Karagiaridi, O. K. Farha and J. T. Hupp, *CrystEngComm*, 2013, **15**, 9258–9264.
9 A. W. Francis, *J. Phys. Chem.*, 1954, **58**, 1099.
10 J. Rouquerol, P. Llewellyn and F. Rouquerol, *Stud. Surf. Sci. Catal.*, 2007, **160**, 49.
11 L. Sarkisov and A. Harrison, *Mol. Simul.*, 2011, **37**(14), 1248; A. Gupta, S. Chempath, M. J. Sanborn, L. A. Clark and R. Q. Snurr, *Mol. Simul.*, 2003, **29**, 29.
12 A. Gupta, S. Chempath, M. J. Sanborn, L. A. Clark and R. Q. Snurr, *Mol. Simul.*, 2003, **29**, 29.
13 O. K. Farha, A. Özgür Yazaydın, I. Eryazici, C. D. Malliakas, B. G. Hauser, M. G. Kanatzidis, S. T. Nguyen, R. Q. Snurr and J. T. Hupp, *Nat. Chem.*, 2010, **2**, 944.

